Electronic Supplementary Material (ESI) for Journal of Materials Chemistry A.


**Fig. S1.** XRD patterns of ZIF-8 and ZIF-8@ZIF-67.

**Fig. S2.** SEM images of (a) ZIF-8 and (b) ZIF-8@ZIF-67.

**Fig. S3.** (a), (b) XRD patterns, (c), (d) SEM and (e), (f) TEM images of ZnSe-NC and $CoSe_2$-NC.

**Fig. S4.** (a) SEM image, (b) TEM image, (c) XRD pattern and (d) HRTEM image of the mesoporous carbon polyhedron after etching.

**Fig. S5.** XRD patterns of (a) the ZIF-8@ZIF-67 processed in Ar atmosphere and (b) after subsequent selenization.

**Fig. S6.** TGA profiles of (a) ZnSe-NC and (b) $CoSe_2$-NC.

**Fig. S7.** Nitrogen adsorption/desorption isotherm of the ZIF-8@ZIF-67. The inset curve shows the corresponding BJH pore size distribution.

**Fig. S8.** Typical CV curves of the (a) ZnSe-NC and (b) $CoSe_2$-NC at a scan rate of 0.2 mV $s^{-1}$ within 0.005-3.0 V for LIBs.

**Fig. S9.** The combined third cycle CV curves of ZnSe-NC, $CoSe_2$-NC and ZnSe-NC@$CoSe_2$-NC for LIBs.

**Fig. S10.** Discharge-charge curves for the initial five cycles of (a) ZnSe-NC and (b) $CoSe_2$-NC at a current density of 0.2 A $g^{-1}$ for LIBs.

**Fig. S11.** (a) Cycling and (b) rate performance of the mesoporous carbon polyhedron obtained by etching of the ZnSe-NC@$CoSe_2$-NC.

**Fig. S12.** SEM images of the ZnSe-NC@$CoSe_2$-NC (a) after 600 discharge and (b) charge cycles. (c), (d) TEM images of ZnSe-NC@$CoSe_2$-NC after 600 cycles.

**Fig. S13.** The long-term cycling performance of the ZnSe-NC@$CoSe_2$-NC anode in another LIBs at a current density of 0.2 A $g^{-1}$.

**Fig. S14.** Non-proportional relation between the square root of scan rate and peak current for LIBs.

**Fig. S15.** Equivalent circuit used for fitting the experimental data of the ZnSe-NC@$CoSe_2$-NC electrode.

**Fig. S16.** GITT curves of (a) ZnSe-NC and (b) $CoSe_2$-NC. $D_{Li+}$ of (c) ZnSe-NC and (d) $CoSe_2$-NC.

**Fig. S17.**The combined third cycle CV curves of ZnSe-NC, $CoSe_2$-NC and ZnSe-NC@$CoSe_2$-NC for SIBs.

**Fig. S18.** Ex-situ TEM/HRTEM images and corresponding SAED patterns of the ZnSe-NC@$CoSe_2$-NC at different discharge-charge stages in SIBs. (a) $100^{th}$ discharge to 0.7 V, (b) $100^{th}$ fully discharge, (c) $100^{th}$ charge to 1.4 V, (d), (e) $100^{th}$ fully charge.

**Fig. S19.** Ex-situ EDX spectrum of the ZnSe-NC@$CoSe_2$-NC electrode collected at various points in SIBs: (a) after first discharging to 0.7 V, (b) after first discharging to 0.005 V, (c) after first charging to 1.4 V, (d) after first charging to 3.0 V.

**Fig. S20.** (a) Cycling performance and (b) rate performance of ZnSe-NC, $CoSe_2$-NC and ZnSe-NC@$CoSe_2$-NC for SIBs.

**Fig. S21.** Kinetics analysis of the electrochemical behavior of the ZnSe-NC@$CoSe_2$-NC nanocomposite for SIBs. (a) CV curves of the ZnSe-NC@$CoSe_2$-NC at various sweep rates. (b) Plots (b-values) of log (scan rate) versus log (peak current) at different oxidation and reduction state. (c) Specifically b value at different oxidation and reduction state. (d) Ratio of the capacitive-controlled charge contribution (shaded area) to the total current at a scan rate of 0.4 mV $s^{-1}$. (e) Ratio of capacitive contribution in

ZnSe-NC@$CoSe_2$-NC at different scan rates. (f) Nyquist plots before and after 50 cycles of the ZnSe-NC@$CoSe_2$-NC.

**Fig. S22.** Non-proportional relation between the square root of scan rate and peak current for SIBs.

**Table S1.** Fitted electrochemical impedance parameters of ZnSe-NC, $CoSe_2$-NC and ZnSe-NC@$CoSe_2$-NC for SIBs.

**Fig. S1.**

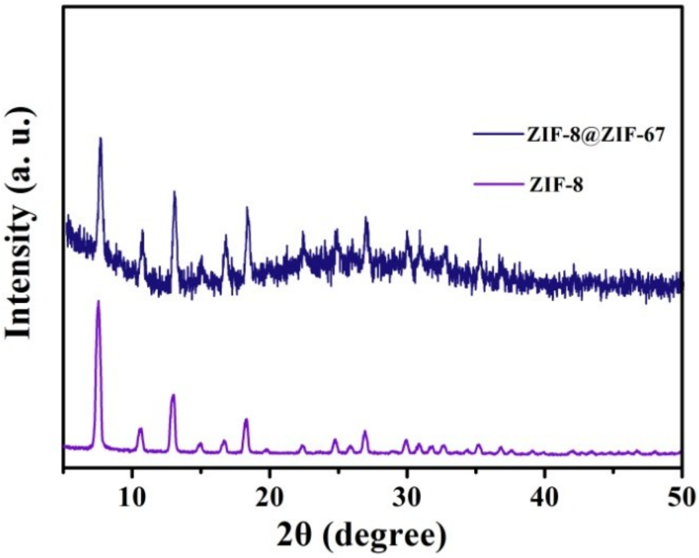

Intensity (a. u.)
ZIF-8@ZIF-67
ZIF-8
10
20
30
40
50
2θ (degree)


**Fig. S2.**

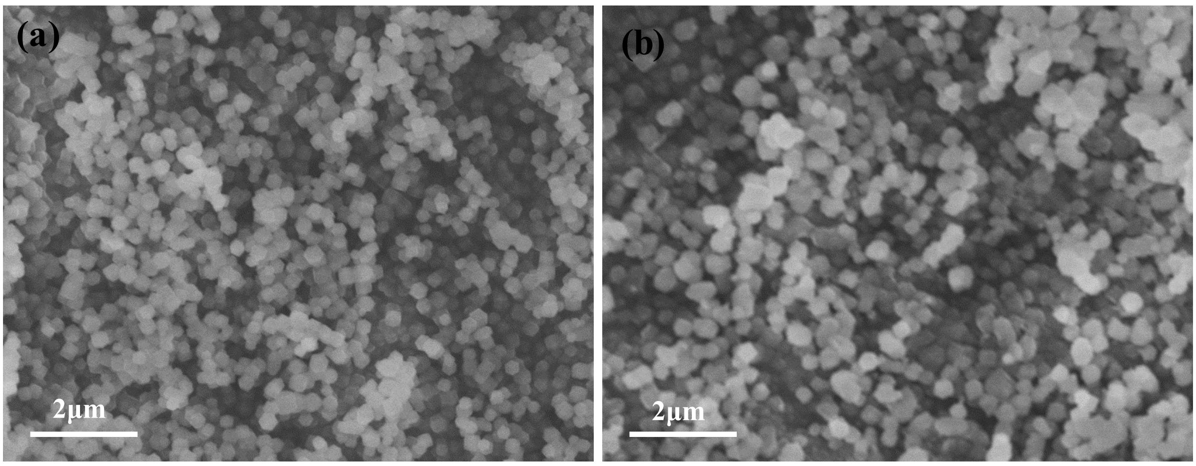

(a)
2μm
(b)
2μm

Fig. S3.

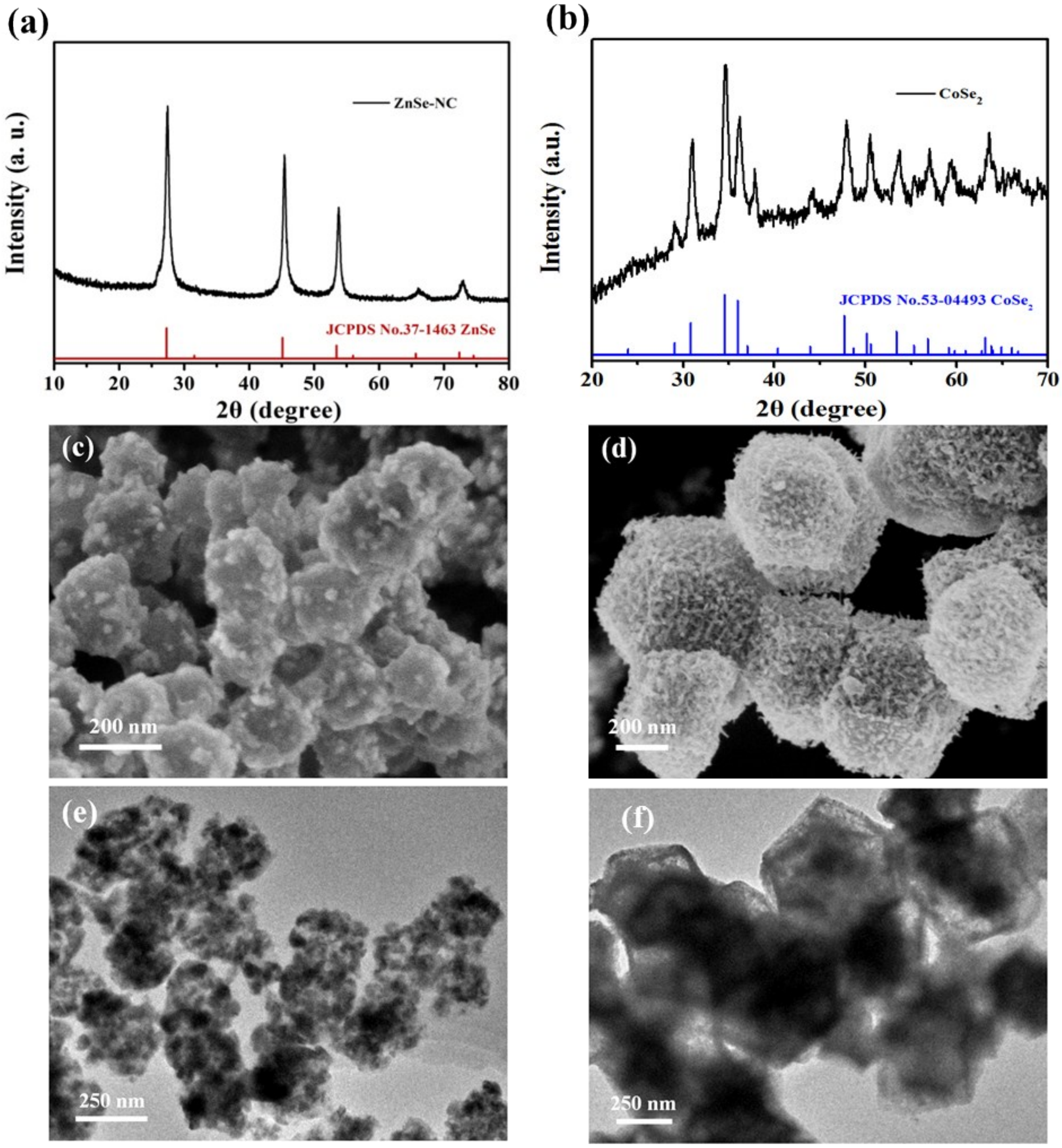

(a)
ZnSe-NC
JCPDS No.37-1463 ZnSe
Intensity (a. u.)
2θ (degree)
10
20
30
40
50
60
70
80
(b)
CoSe2
JCPDS No.53-04493 CoSe2
Intensity (a.u.)
2θ (degree)
20
30
40
50
60
70
(c)
200 nm
(d)
200 nm
(e)
250 nm
(f)
250 nm

**Fig. S4.**

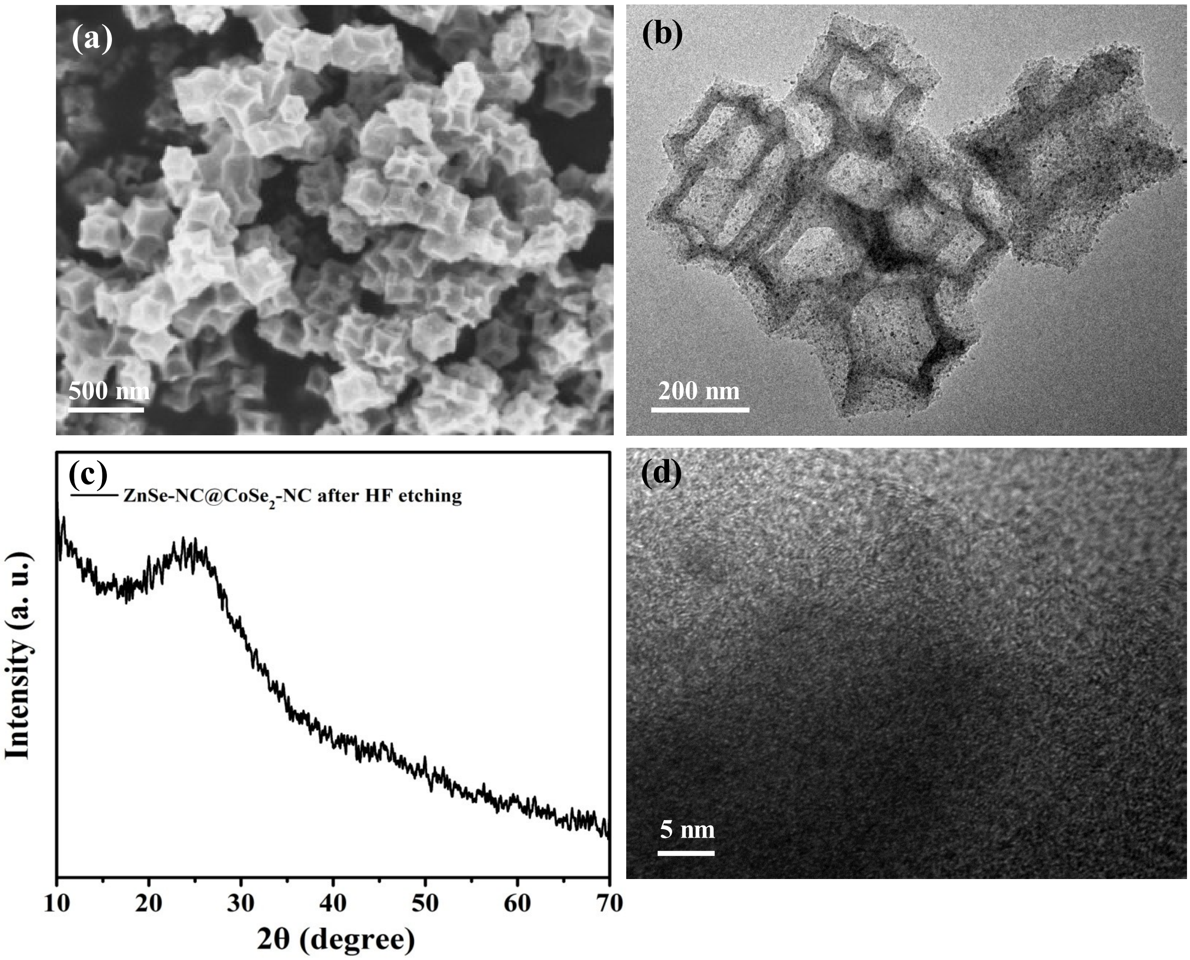

(a)
500 nm
(b)
200 nm
(c)
ZnSe-NC@CoSe$_2$-NC after HF etching
Intensity (a. u.)
2θ (degree)
(d)
5 nm


**Fig. S5.**

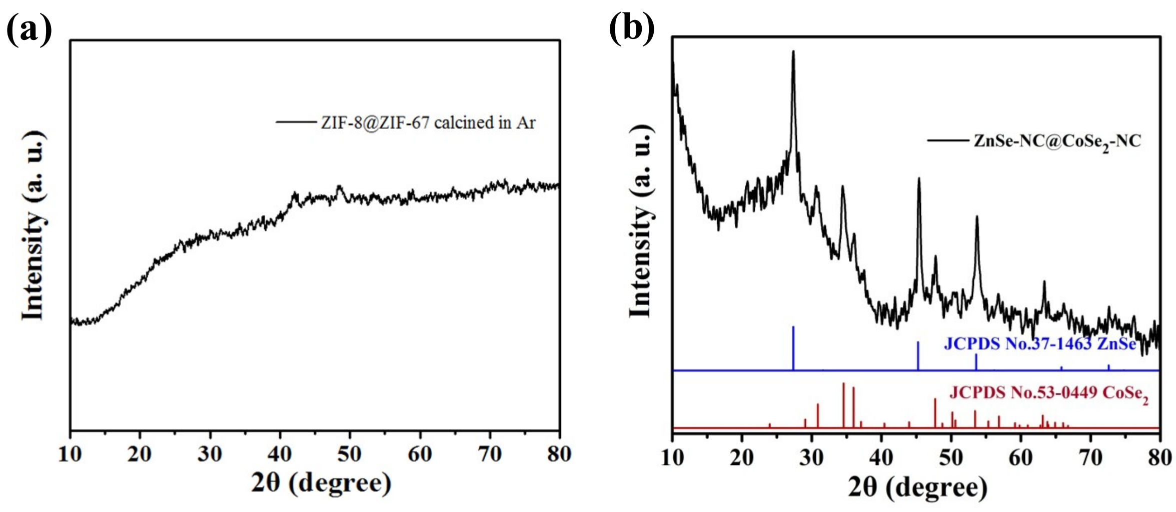

(a)
ZIF-8@ZIF-67 calcined in Ar
Intensity (a. u.)
2θ (degree)
(b)
ZnSe-NC@CoSe$_2$-NC
JCPDS No.37-1463 ZnSe
JCPDS No.53-0449 CoSe$_2$
Intensity (a. u.)
2θ (degree)

**Fig. S6.**

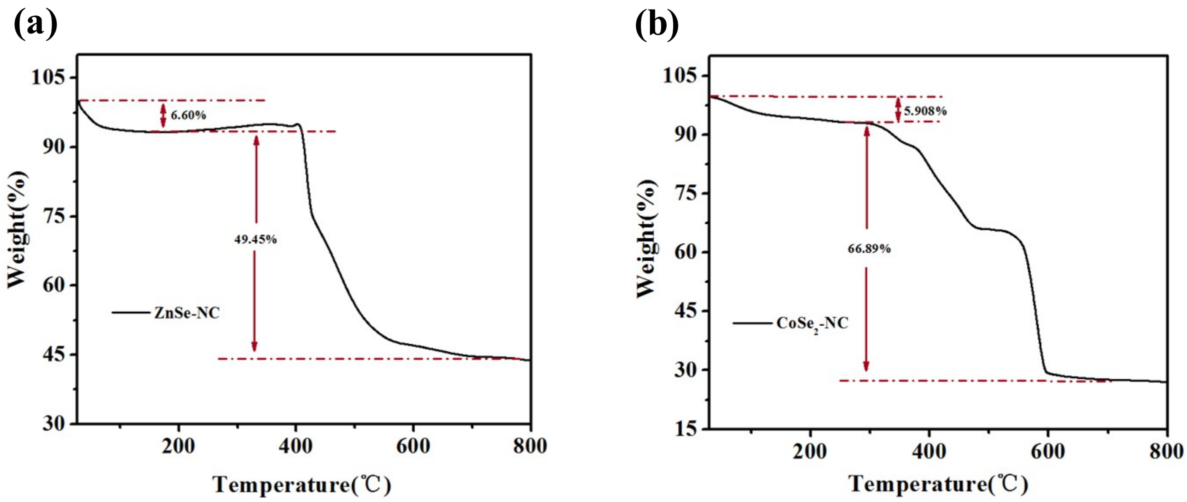


When the ZnSe-NC@$CoSe_2$-NC nanocomposite was heated at the temperature range of 25 to 800 °C, the phases of the components in the composite were transformed according to the following reactions:

$$ZnSe\ (s) + O_2\ (g) \rightarrow ZnO\ (s) + SeO_2\ (g) \qquad (1)$$

$$3CoSe_2\ (s) + 8O_2\ (g) \rightarrow Co_3O_4\ (s) + 6SeO_2\ (g) \qquad (2)$$

$$C\ (s) + O_2\ (g) \rightarrow CO_2\ (g) \qquad (3)$$

In the ZnSe-NC@$CoSe_2$-NC nanocomposite, the mass ratios of ZnSe, $CoSe_2$ and N-doped carbon can be denoted as $x$, $y$ and $z$, respectively and the addition of $x$, $y$ and $z$ value equals 100%. As we know, the ZnSe-NC@$CoSe_2$-NC was obtained by the selenization of ZIF-8@ZIF-67 polyhedrons. So, the N-doped carbon in the ZnSe-NC@$CoSe_2$-NC is from the ZIF-8 and ZIF-67. In order to get $x$, $y$ and $z$ value, besides the TGA curve of ZnSe-NC@$CoSe_2$-NC, the TGA curves of ZnSe-NC and $CoSe_2$-NC were also obtained. Based on the reaction (1) and the corresponding TGA of ZnSe-NC in Fig. S6a, the theoretical loss ratio of ZnSe is (100-81/144) % = 43.8% and the ratio of ZnSe to N-doped carbon is 78.13%/21.87%. Based on the reaction (2) and the corresponding TGA of $CoSe_2$-NC in Fig. S6b, the theoretical loss ratio of $CoSe_2$ is [100-240.79/(216.85 × 3)] % = 62.9% and the ratio of $CoSe_2$ to N-doped carbon is 73.49%/26.51%. According to above analysis and the data in Fig. 3b, we can get the three equations of $x$, $y$ and $z$.

$x + y + z = 100\%$,

$43.8\%x + 62.9\%y + z = 58.11\%$,

$(21.87\%/78.13\%)x + (26.51\%/73.49\%)y = z$

As a result, the content of ZnSe, $CoSe_2$, N-doped carbon is 68.8%, 8.8% and 22.4%, respectively.

**Fig. S7.**

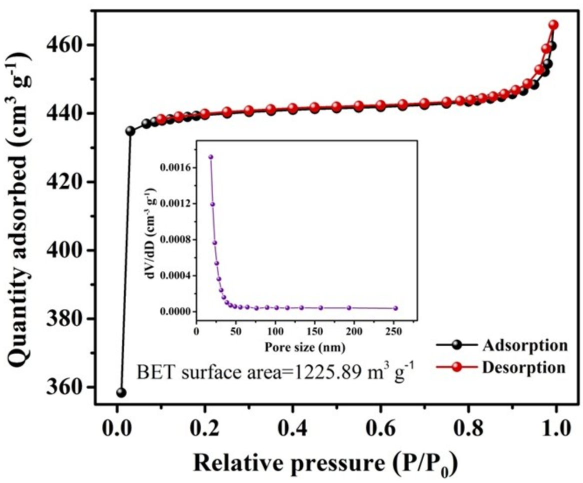

Fig. S8.

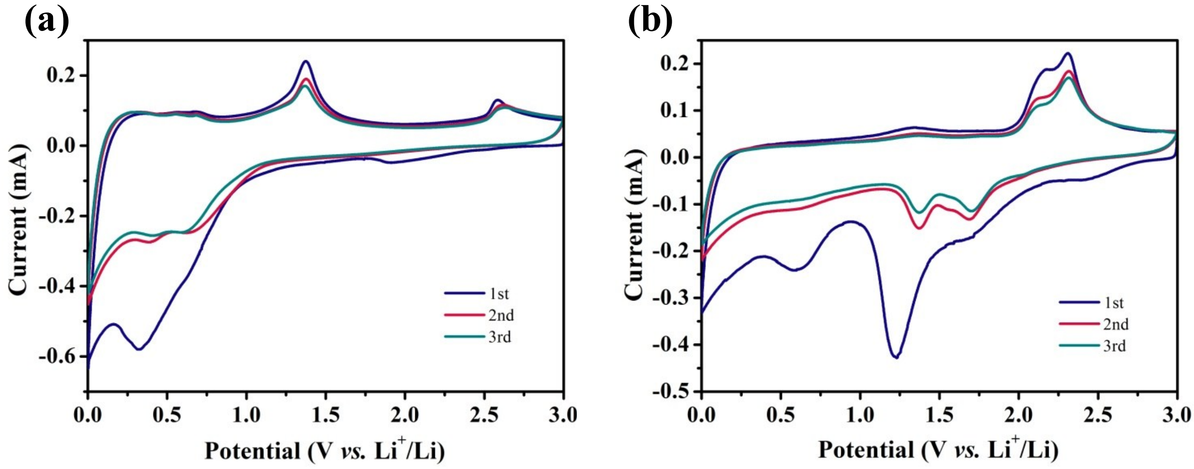
(a)
Current (mA)
Potential (V vs. Li+/Li)
1st
2nd
3rd
(b)
Current (mA)
Potential (V vs. Li+/Li)
1st
2nd
3rd

Fig. S9.

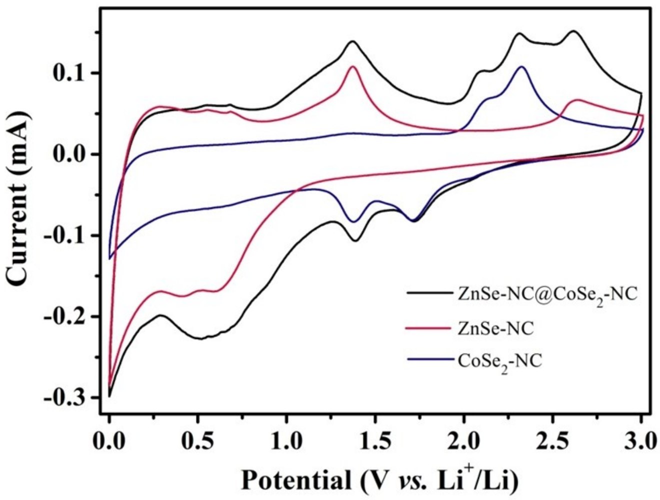
Current (mA)
Potential (V vs. Li+/Li)
ZnSe-NC@CoSe2-NC
ZnSe-NC
CoSe2-NC

Fig. S10.

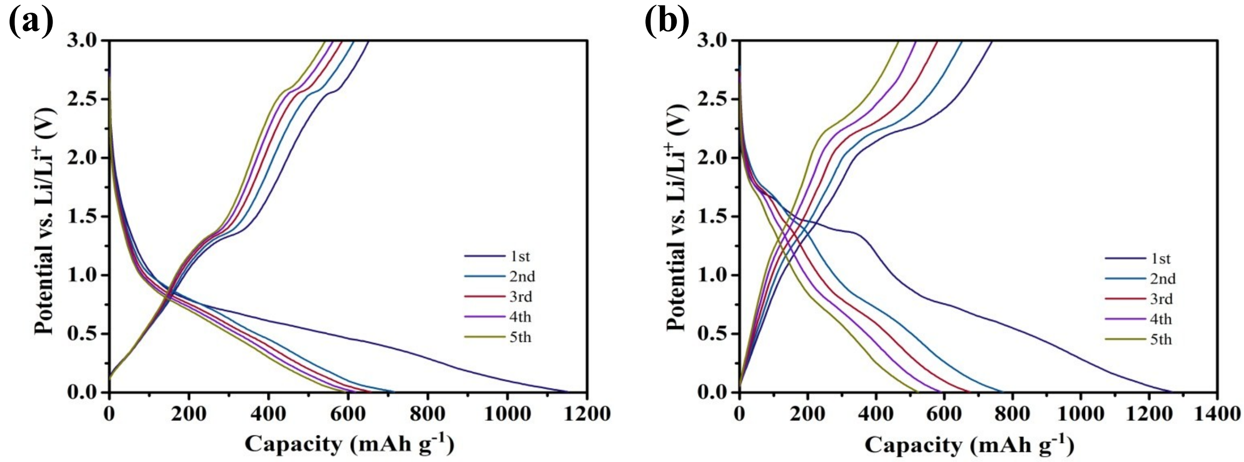


Fig. S11

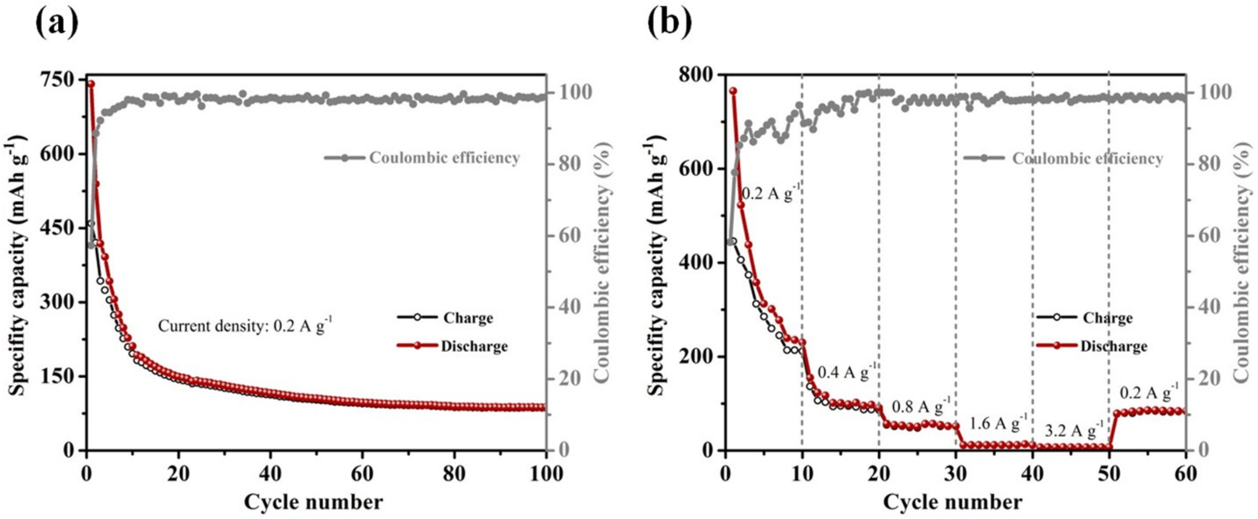

**Fig. S12.**

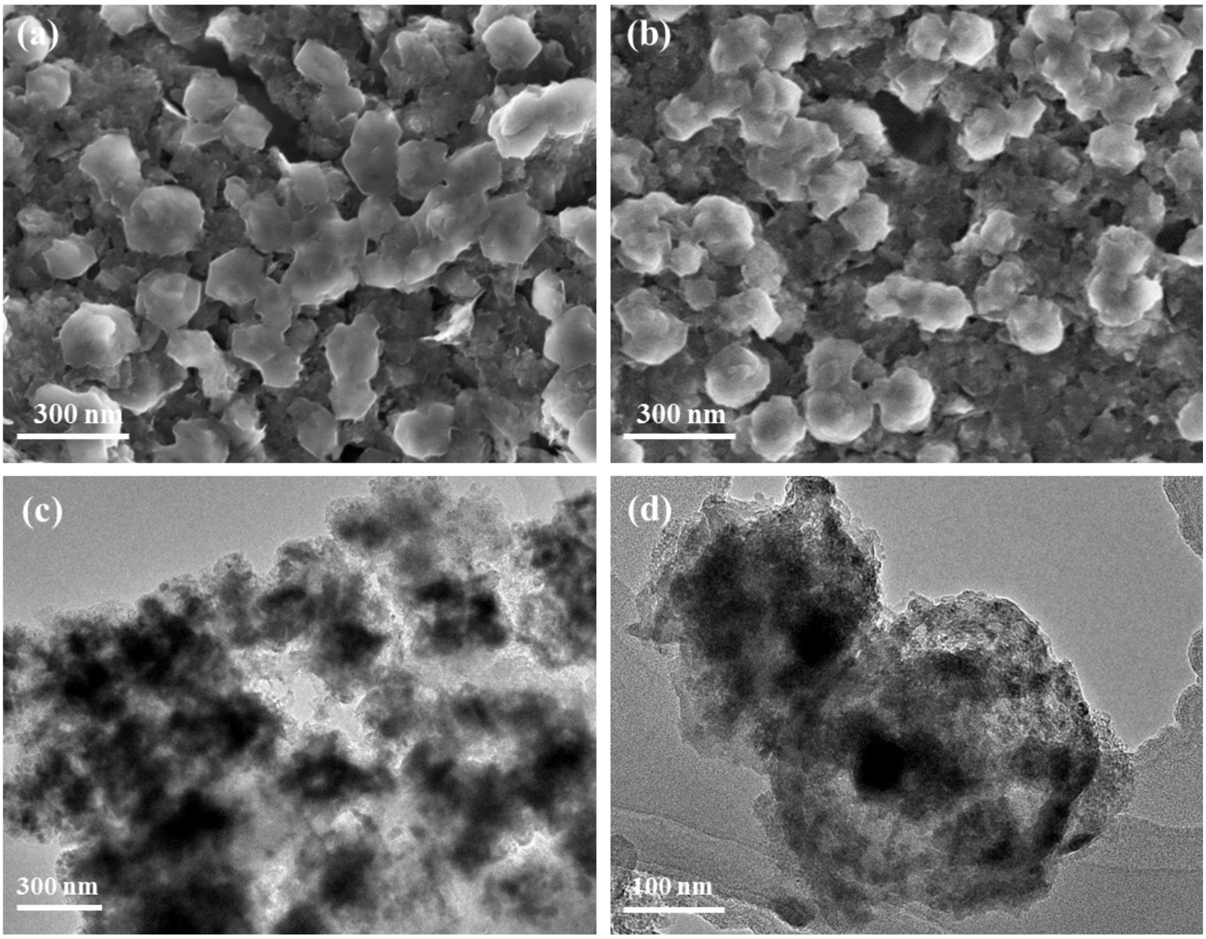

Fig. S13.

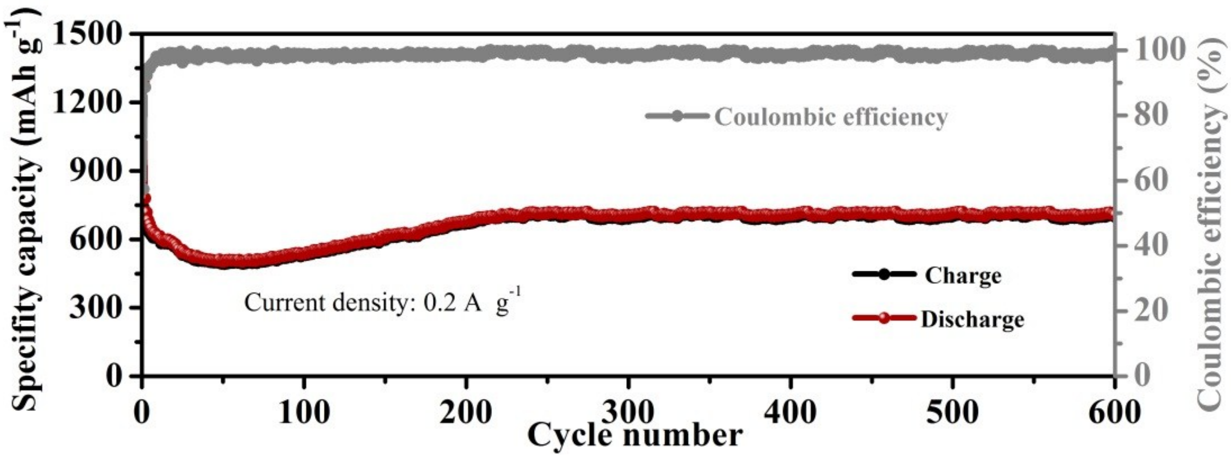


Fig. S14.

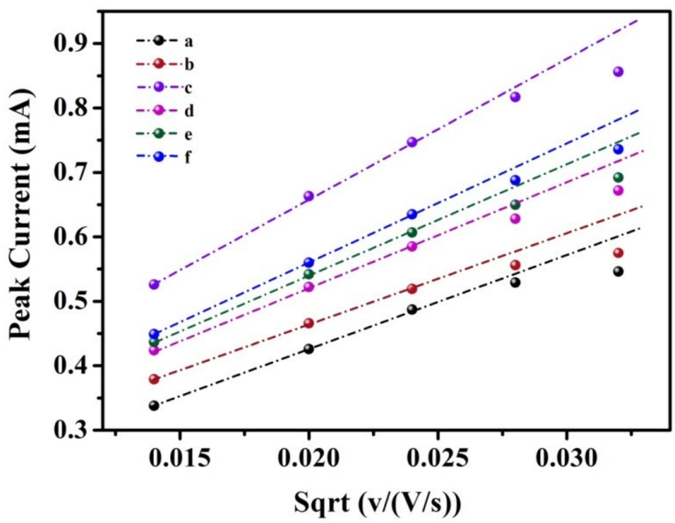


Fig. S15.

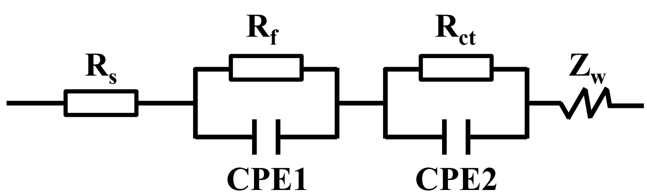

Fig. S16.

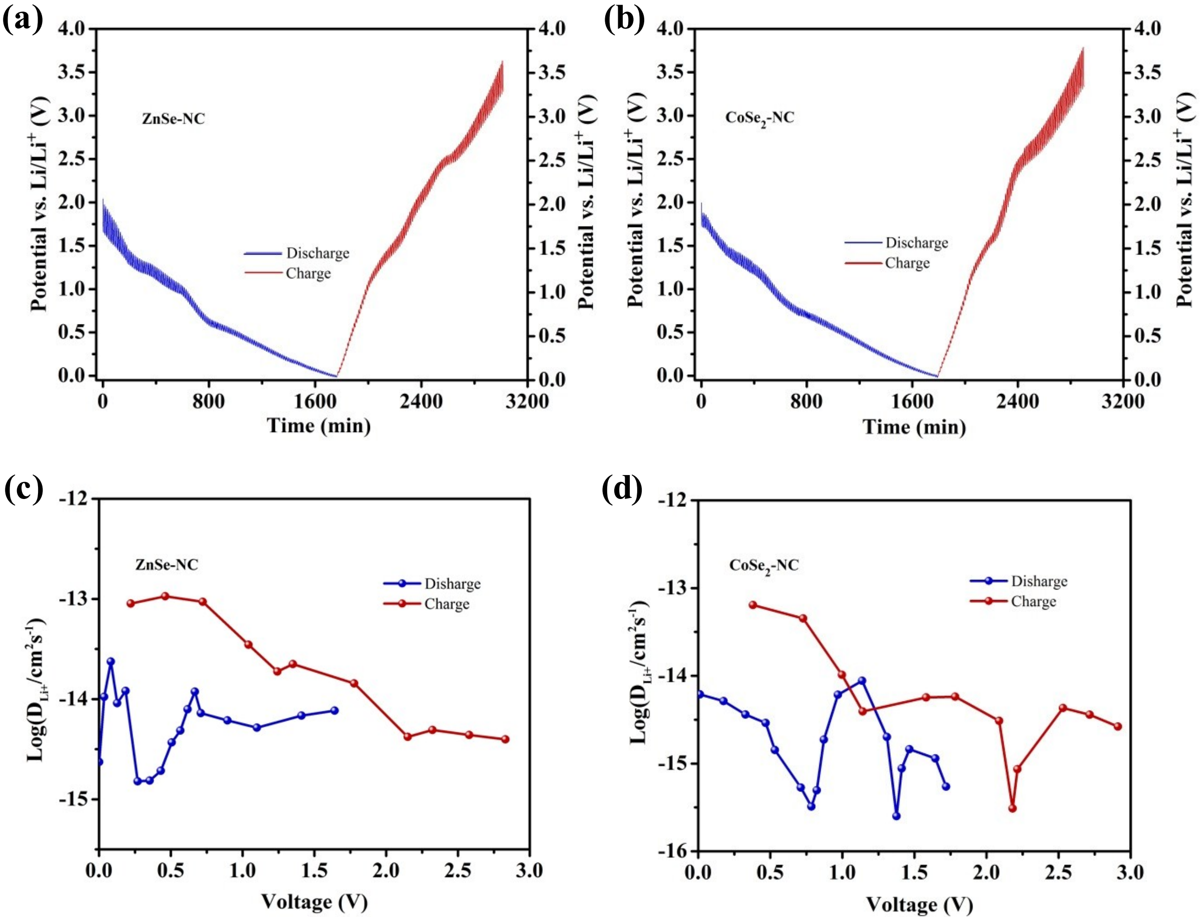


Fig. S17.

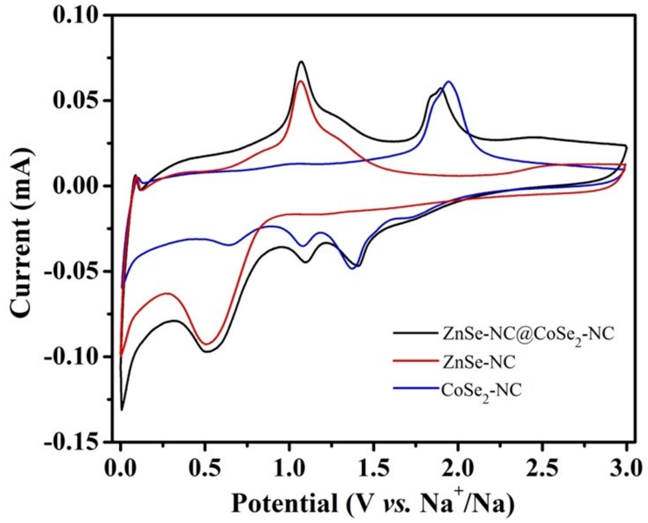

**Fig. S18.**

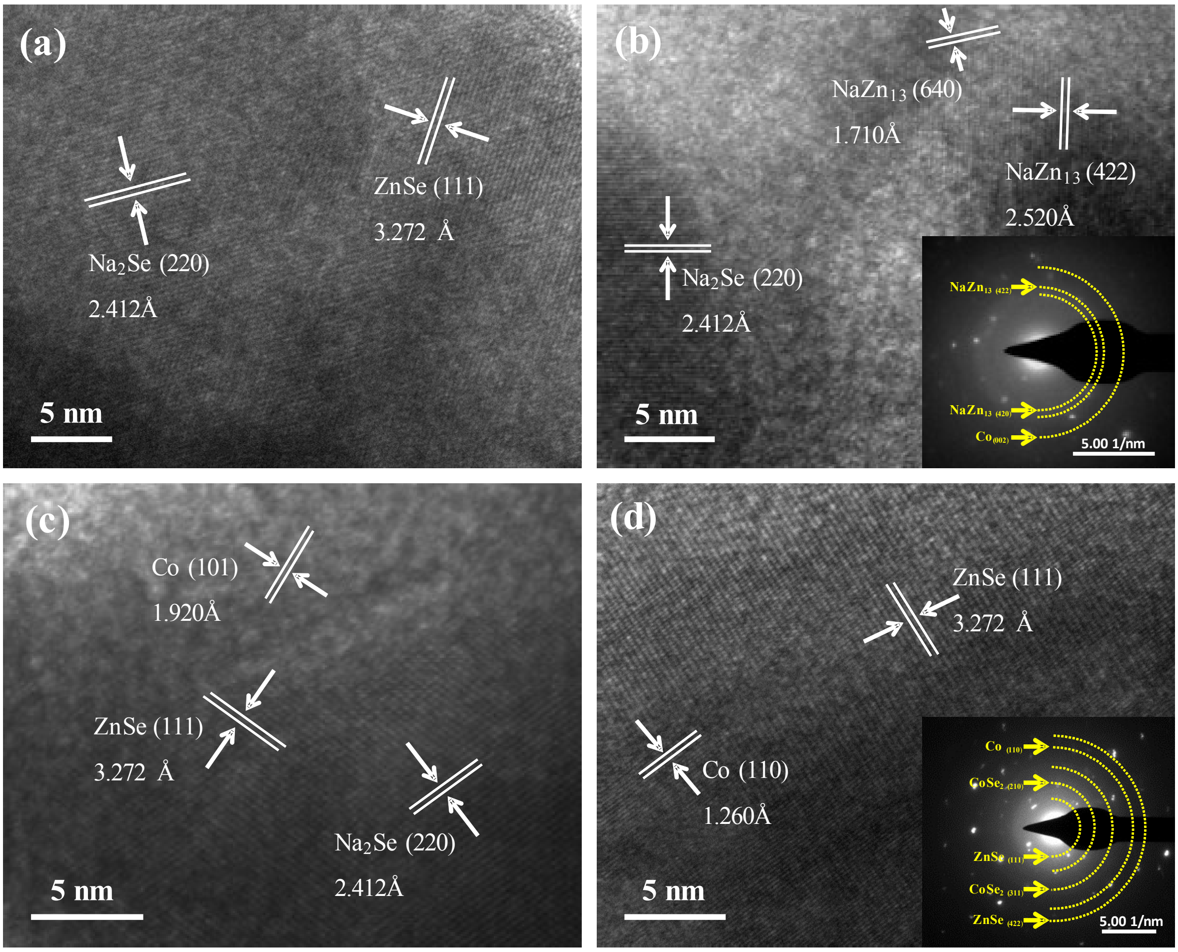

(a)
Na2Se (220)
2.412Å
ZnSe (111)
3.272 Å
5 nm
(b)
NaZn13 (640)
1.710Å
NaZn13 (422)
2.520Å
Na2Se (220)
2.412Å
5 nm
NaZn13 (422)
NaZn13 (420)
Co (002)
5.00 1/nm
(c)
Co (101)
1.920Å
ZnSe (111)
3.272 Å
Na2Se (220)
2.412Å
5 nm
(d)
ZnSe (111)
3.272 Å
Co (110)
1.260Å
5 nm
Co (110)
CoSe2 (210)
ZnSe (111)
CoSe2 (311)
ZnSe (422)
5.00 1/nm

**Fig. S19.**

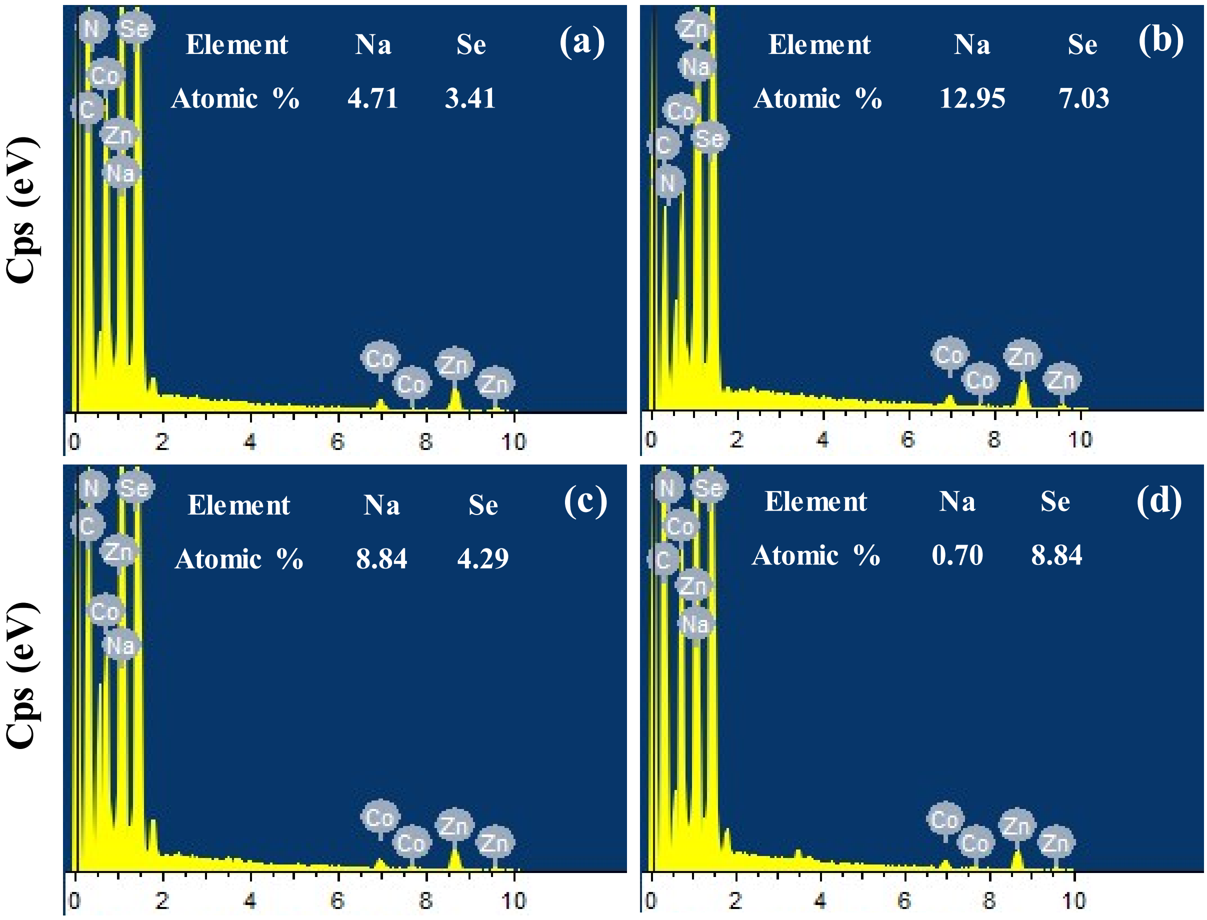


**Fig. S20.**

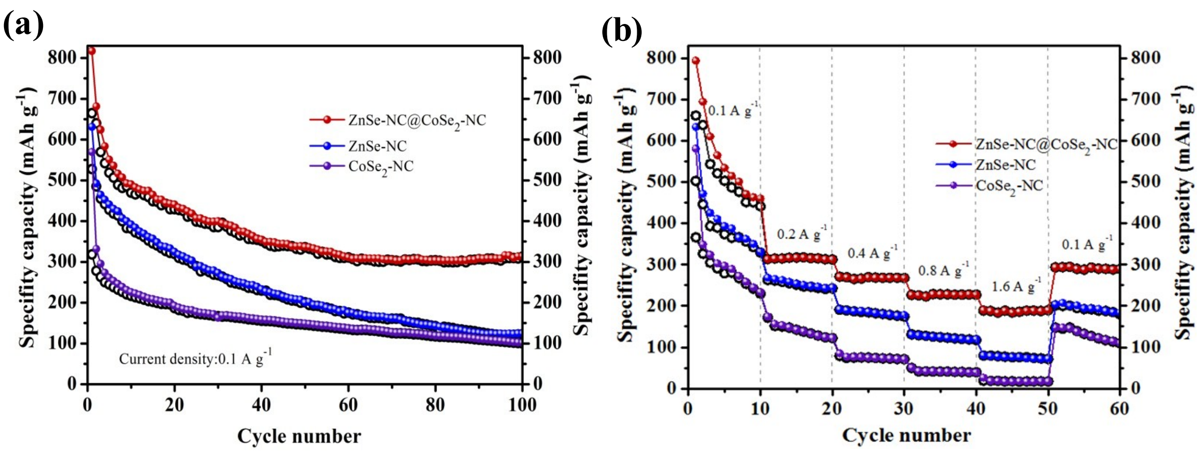

## Fig. S21.

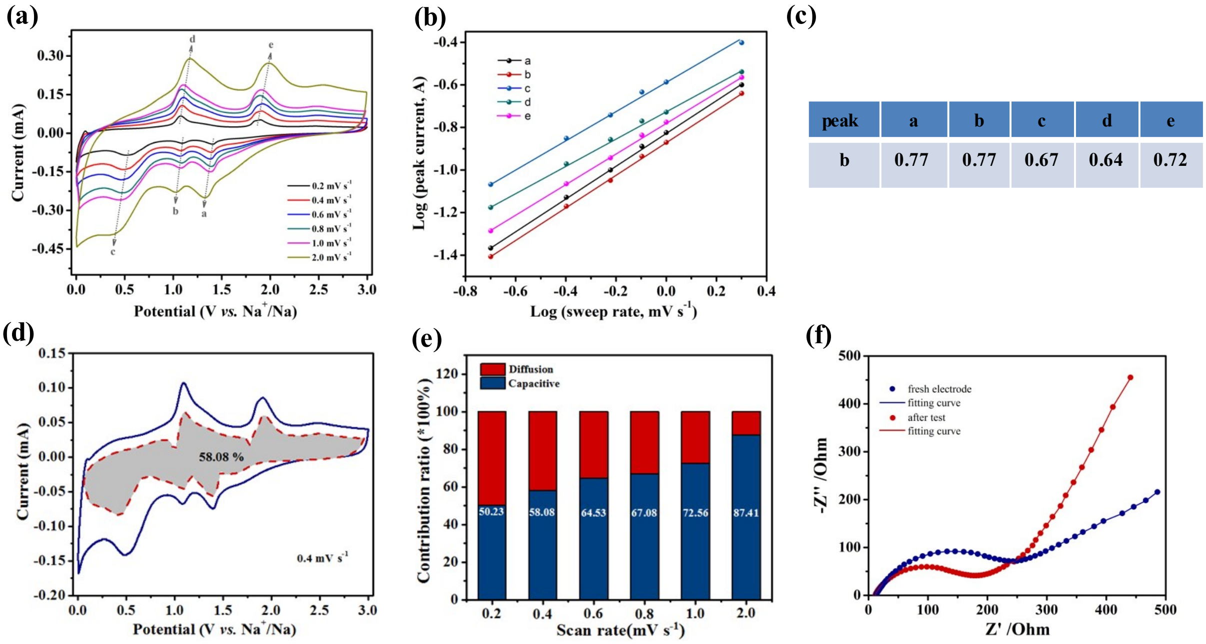


| peak | a | b | c | d | e |
|---|---|---|---|---|---|
| b | 0.77 | 0.77 | 0.67 | 0.64 | 0.72 |

## Fig. S22.

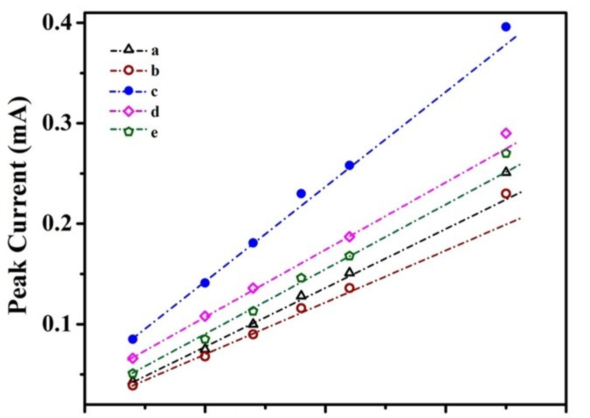


## Table S1.

| Sample | State | $R_s$ (Ω) | $R_f$ (Ω) | CPE1 (μMΩ) | $R_{ct}$ (kΩ) | CPE2 (mMΩ) | $Z_w$ (mMΩ) |
|---|---|---|---|---|---|---|---|
| ZnSe-NC @$CoSe_2$-NC | fresh | 12 | 197 | 15.2 | 11 | 17.3 | 3.27 |
| | after test | 11 | 157 | 21.5 | 9.9 | 14.4 | 1.23 |